ELSEVIER

Polymer 43 (2002) 1277–1285

polymer

www.elsevier.com/locate/polymer

Determination of thermal stress distribution in a model microelectronic device encapsulated with alumina filled epoxy resin using fluorescence spectroscopy

Naoki Muraki*, Nobuhiro Matoba, Takayuki Hirano, Masanobu Yoshikawa

[a]*Material Science Laboratory, Toray Research Center, Inc., Sonoyama 3-3-7, Otsu, Shiga 520-8567, Japan*

Received 3 April 2001; received in revised form 24 August 2001; accepted 15 October 2001

Abstract

A method for measuring residual and applied stresses in particulate polymer systems, which utilizes the piezo-spectroscopic effect of the optical fluorescence of filled particles, is presented. Fluorescence piezo-spectroscopy (PS) is non-destructive and provides microscopic lateral resolution upon using an optical microprobe system. Epoxy resin filled with α-alumina particles is used in this study. Stress values are obtained by frequency shift measurement of the characteristic optical fluorescence lines produced by Cr^{3+} impurities in alumina. The relationships between peak frequency shift of these lines and stress are derived by using a 4-point-bending test. The peak frequency shift shows linear correlation with tensile stress, while a non-linear relation between peak frequency shift and stresses is found in the compressive stress region. To a first order approximation, residual stresses were calculated by the frequency shift divided by the linear correlation coefficient in the tensile stress region. As an application of the PS method, we determined micron order residual stress distributions in a model plastic encapsulated silicon substrate for microelectronic devices and compared the stress data with those calculated using a two-dimensional finite element analysis of the device. The experimental results were in good agreement with the tensile stress components that have been obtained by theoretical calculation. Therefore, PS techniques can be used to measure residual stresses in polymer compounds utilizing the information obtained from the fluorescence lines of a dispersed ceramic powder.

Keywords: Piezo-spectroscopy; Epoxy-molding resin; Thermal residual stress

1. Introduction

The modern semiconductor industry utilizes resin-encapsulated diodes, transistors, ICs, LSI, and super LSIs. Among various resin compounds for encapsulating semiconductor devices, epoxy-molding compounds added with inorganic particles are rather frequently employed, owing to a suitable combination of mechanical, electrical and thermal properties [1–3]. However, epoxy-molding compounds cured at elevated temperatures yield appreciable thermoelastic residual stresses. Pronounced stresses can therefore be generated within the device as a result of a mismatch in thermal expansion coefficient [4]. These thermal stresses might give rise to device failure, including package cracking, Al pattern deformation, passivation microcracking and chip cracking [5–9]. The trend of semiconductor devices is toward an increasingly higher degree of integration, forcing the design toward larger chips, finer patterns, and higher pin counts that are more susceptible to internal stress failure. Packages, on the other hand, are designed to be small and thin to meet the demands for lightweight and compact devices in electronic equipment. Stress management, therefore, has been an essential aspect of microelectronics manufacturing and stress estimation has increasingly become a matter of great importance. Furthermore, since the internal stresses in the encapsulant resin must be concentrated near the interface or at the edges of the contact material, knowledge of residual stresses on a microscopic scale has long been a deep concern for manufacturers [4].

Although several techniques have been utilized for the measurement of residual stress, almost all the techniques have their own limitations, especially, in terms of the spatial resolution. Conventional strain gauge methods widely used for stress measurement in various materials can also be applied to polymeric systems, but its spatial resolution is limited to the order of several millimeters. Photoelastic analysis, which is a powerful technique to obtain residual stress distributions in polymeric materials, can only be

* Corresponding author. Tel.: +81-775-533-8608; fax: +81-775-533-8696.

E-mail address: naoki_muraki@trc.toray.co.jp (N. Muraki).

0032-3861/02/$ - see front matter
PII: S0032-3861(01)00691-7

applied to opaque and flat shaped resins [10,11]. X-ray diffraction [12–14], which is an elegant and direct method for stress detection in single crystals and polycrystalline materials, can only be applied to crystals and cannot be used for direct stress measurements in amorphous polymers like epoxy resins. Additionally, X-ray techniques have insufficient spatial resolution to study residual stresses at interfacial regions on a micrometer scale.

An alternative method of measuring stresses is piezo-spectroscopy (PS) which utilizes the frequency shift of characteristic luminescence lines (Raman or fluorescence) with stress [15–20]. One of the most important advantages of PSs is in their high spatial resolution of a few microns or less in diameter, since the exciting laser beam can be focused on samples with an optical microscope. Therefore, this technique has been widely used for microscopic stress investigations in semiconductor materials [15,16], ceramics [17,18], corrosion scales [19], and composite materials [20]. However, PS has also severe limitations when applied to polymeric materials, which usually do not have sufficiently sharp and intense Raman bands to allow the peak shift with stress to be measured precisely. To make matters worse, commonly used thermosetting resins have broad fluorescence lines, which usually interfere with the measurement of fine Raman spectra.

In this paper, we present a new technique of measuring residual stresses in particulate polymer systems by using the optical fluorescence of filler particles. The alumina filled epoxy resin used in this research may be one instructive system for the illustration of this technique. Ruby fluorescence relies on the incorporation of Cr^{3+} into α-Al_2O_3, which fortunately occurs naturally in alumina powders [21]. Furthermore, the efficiency of ruby fluorescence is so high that a sufficient fluorescence signal can easily be obtained from alumina filler even in a cured epoxy matrix regardless of its own broad fluorescence line. This prominent ruby fluorescence has been used for decades as a stress indicator in diamond anvil cells [22]. More recently, it has been applied to measure both residual and external stresses of a variety of forms of α-alumina, such as single crystal sapphire [23], alumina ceramics [24], ceramic composites [25], and resin matrix composites reinforced with alumina-based fibers [26]. In this paper, we have applied the ruby fluorescence to stress determination in a polymeric material filled with alumina particles. As a first step, we have investigated the stress dependence of fluorescence lines from alumina powder embedded in epoxy resin compound. It is very important to precisely know the stress correlation with frequency shift, before attempting a quantitative stress analysis by PS. A 4-point-bending test was used for such a preliminary investigation. The final aim of this study is to illustrate the suitability of the PS technique in determining microscopic residual stress distributions in encapsulated semiconductor devices. This goal is pursued by comparing experimental results of PS with theoretical calculations obtained using the finite element method (FEM).

2. Piezo-spectroscopy

In a first-order approximation, the stress dependence of a band position is given by the following tensorial expression [24]

$$\Delta\nu = \Pi_{ij}\sigma_{ij} \tag{1}$$

where $\Delta\nu$ is the peak frequency shift, σ_{ij} is the stress tensor and Π_{ij} is the matrix of the PS coefficients. This equation is correct for stresses applied in the crystallographic reference frame of the material under investigation. In the case of Cr^{3+} doped α-alumina, the stress dependence of the transition for this material has been investigated in the literature. According to the results of precise measurement of a single crystal [27], the off-diagonal components of PS coefficients for α-alumina are found to be almost zero and can be neglected. It was found that the shift $\Delta\nu$ of the R_1 and R_2 transitions depend on the axial stress tensor, referred to the crystallographic axes of Al_2O_3, according to the following relations [27]:

$$\Delta\nu(R_1) = 2.56\sigma_{11} + 3.50\sigma_{22} + 1.53\sigma_{33} \tag{2}$$

$$\Delta\nu(R_2) = 2.66\sigma_{11} + 2.80\sigma_{22} + 2.16\sigma_{33} \tag{3}$$

where the coefficients of σ_{11}, σ_{22} and σ_{33} in Eqs. (2) and (3) are the PS coefficients, in units of cm^{-1} GPa^{-1}. For the more general case of a stress tensor randomly oriented, a transformation matrix is required. In the case of polycrystalline samples or/and particles in plastics, the tensor expression loses its meaning. However, also in this case, the measured frequency shift of the stressed material, $\langle\Delta\nu\rangle$, can be expressed by the relationship:

$$(\sigma_1 + \sigma_2 + \sigma_3) = 3\langle\Delta\nu\rangle/\Pi_{tr} \tag{4}$$

where Π_{tr} is the trace of the PS tensor and σ_1, σ_2 and σ_3 are the principal stress components. In the general case, it is not possible to deduce individual stress components from a fluorescence spectrum and this is one of the major limitations of PS. In other words, the frequency shift gives only a cumulative information of the principal stress components. In general, it is necessary to calculate the expected sum of the stress components from an assumed or calculated stress distribution (e.g. from FEM) in order to compare those with the measured one. If a uniaxial stress, σ_{uni}, is applied to a polycrystalline substance, the relationship can be expressed using an average of the diagonal PS tensor, $\Pi_{ave} = \Pi_{tr}/3$

$$\sigma_{uni} = \langle\Delta\nu\rangle/\Pi_{ave} \tag{5}$$

As far as the stress dependence in a 4-point-bending test is concerned, applied stresses at the center of the sample can be regarded as uniaxial and changing linearly from compression to tension. Hence, Eq. (5) is exact and can be used to determine the average PS coefficient, Π_{ave}.

3. Experimental

3.1. Material

The epoxy resin used in this study was commercially available Bisphenol-A type (Epikote828, epoxide equivalent: 190 ± 5) obtained from Yuka Shell Epoxy KK. The hardener, dicarboxylic acid (YH300) was also received from the same company. Triphenylphosphine (TPP) as catalyst was used as received from Nacalai tesque Inc. The epoxy resin used in this study is composed of a weight ratio, 1:0.8 of epoxy and a hardener, and the content of TPP is 1 phr (part per hundred resin). α-Alumina powder with average particle size of 12 μm was also purchased from Nacalai tesque Inc. Two kinds of sample were prepared for measuring the stress dependence of fluorescence spectra; one contained an alumina filler treated with silane coupling agent and the other contained a non-treated alumina filler. Both samples were manufactured using exactly the same process except for the silane treatment. Silane coupling agent (SH6040, γ-(amino-ethyl)-aminopropyltrimethoxy silane) used as a primer was obtained from Dow Corning Toray Silicone Co. Regarding the silane surface treatment, the alumina powder was immersed in a water solution that contained 0.1% silane for 15 min and then heated in an oven at 120 °C for 3 h. Alumina filler was mixed with the epoxy resin at ambient temperature, the concentration of the filler being 65 wt%. After mixing, the samples were placed in a vacuum oven for about 1 h to remove entrapped air. These samples were put on glass plates coated with poly-(tetrafluoroethylene) (PTFE) films. The two-step curing cycle lasted for 3 h at 80 °C and 6 h at 150 °C. After curing, the samples were allowed to cool slowly in the oven. Cured samples were sliced with a diamond saw into bars ($=40\times8\times4$ mm) for 4-point-bending tests and measurement of other mechanical properties, and the surfaces of the specimens were polished with 0.5 μm diamond paste. A universal-testing machine (Model 1185, Instron Co.) and strain gauges were used for the measurement of Young's modulus and Poisson's ratio of cured samples at room temperature. A thermomechanical analyzer, TMA (CN8098D1, Rigaku Co.) was used to obtain the thermal expansion coefficient in the temperature range 20–150 °C. The glass transition temperature of the filled resin was 125 °C, as measured from the temperature of the inflection point in the thermal expansion curve obtained by TMA.

A simple, plastic-encapsulated microelectronic device was also manufactured using the same procedure. A silicon substrate ($=5\times5\times0.3$ mm) was molded in the degassed resin and cured between two glass plates coated with PTFE film. The curing procedure was carried out as previously described. Cured samples were cut at the center of the Si substrate. The surface of the cross-section was polished with 0.5 μm diamond paste. A cross-section of the model sample is shown schematically in Fig. 1. Although this model contain neither electrical circuits nor wiring, it is sufficient to evaluate the residual stress distribution in the resin around the Si substrate and to know the relationship between residual stresses in the resin and the mechanical properties of the package.

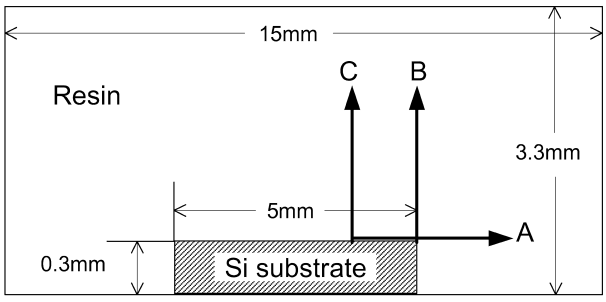

Fig. 1. Schematic showing the cross-section structure of the encapsulate model microelectronic device. Arrows A–C denote the specific scanned lines.

3.2. Fluorescence spectroscopy

A commercially available Raman spectrometer (T-64000 Jobin Yvon Ltd/Horiba group, Tokyo, Japan) was used for fluorescence measurements without further modification. In the case of 4-point-bending experiments, the exciting laser was focused onto samples with an optical lens and a small mirror in the back scattering configuration. An argon ion laser, operating at a wavelength of 514.5 nm with a power of 5 mW on sample, was used as an excitation source. The size of the probe beam was about 100 μm. A camera lens was used to collect the scattered light, which was then analyzed with a monochromator; a single monochromator option was employed, equipped with a charge coupled device (CCD) detector. After the load was applied, spectra were recorded using a step size of 200 μm from the compressive side toward the tensile side of the bend bar. The polarization of incident light was parallel to the direction of uniaxial stress. Induced stress values at the measured points were calculated from a standard formula for 4-point-bending.

An optical microprobe was used for the measurement of the local residual stress distribution in the encapsulant of the model microelectronic device. The excitation laser was focused onto the sample with an optical microscope, and the same objective lens (×20) was used to collect the scattered light. The dimension of the laser spot on sample was about 5 μm. A cross-slit was used to cut the scattered light from the defocused region. The effective depth of the microprobe measurement could be roughly controlled by changing the dimension of the cross-slit. In the present work, the cross-slit was kept at 1 mm and the effective observation depth was about 30 μm. The laser irradiation time was about 3 s per spectrum. Preliminary experiments showed that there were small shifts of the peaks due to laser heating. An almost linear correlation was found between peak shift and incident laser power. These heating effects

were ignored, because the laser power and other experimental conditions were identical throughout all experiments. Instrumental fluctuations were compensated for by monitoring a spontaneous emission line (14,355 cm^{-1}) from the Ar^+ laser. A heating stage (LIKAM TH600, Japan High Tech KK) for the optical microscope was used for the measurements of stress distributions at high temperature. The recorded spectra were manipulated with commercially available software (Grams/386, Galactic Ind. Co.). In order to obtain precise peak frequencies for each fluorescence band, the spectra were decomposed with two Lorenzian line shapes for fluorescence bands and one gaussian line shape for the spontaneous emission line of the Ar^+ laser.

3.3. Theoretical stress calculation

The residual stress was considered to be caused mainly by a mismatch in thermal expansion coefficients between the silicon substrate and the resin, when these were cooled down from the glass transition temperature (T_g) to room temperature. Applied stresses in the epoxy resin might relax because the motions of epoxy molecular chains do not freeze out at temperatures higher than T_g [28]. Due to a larger coefficient of thermal expansion in alumina/epoxy resin than in the Si substrate, the resin is in a compressive stress state upon cooling down to ambient temperature (T_a). The thermal elastic stress of the resin in the vicinity of the Si substrate is given by the elastic two-layer model [29]:

$$\sigma_{th} = E_r \int_{T_g}^{T_a} (\alpha_r(T) - \alpha_s(T))dT \quad (6)$$

where E_r and v_r are the alumina/epoxy resin Young's modulus and Poisson's ratio, respectively. $\alpha(T)$ is a function of the thermal expansion coefficient. Here, suffix 'r' and 's' are used to denote the resin and Si substrate, respectively. Moreover, when average thermal coefficients are taken into account, the expression becomes

$$\int_{T_g}^{T_a} \alpha(T)dT = \bar{\alpha}(T_g - T_a) \quad (7)$$

Thus, the residual stress in the resin in the vicinity of the Si substrate (i.e. induced during the cooling procedure) is simply proportional to the Young's modulus of the resin, to the mismatch between the thermal expansion coefficients of resin and Si, and to the difference between the glass transition temperature and atmospheric temperature.

FEMs were used to calculate the residual stresses caused by a change from stress-free condition at the glass transition temperature to ambient temperature in the specimens, alumina/epoxy resin and Si substrate were assumed to be perfectly bonded. A two-dimensional model, under a plane-strain hypothesis, was employed for the FEM calculation. A schematic model of the plastically encapsulated microelectronic device is shown in Fig. 1. Only half of the model was meshed because of symmetry. The computational

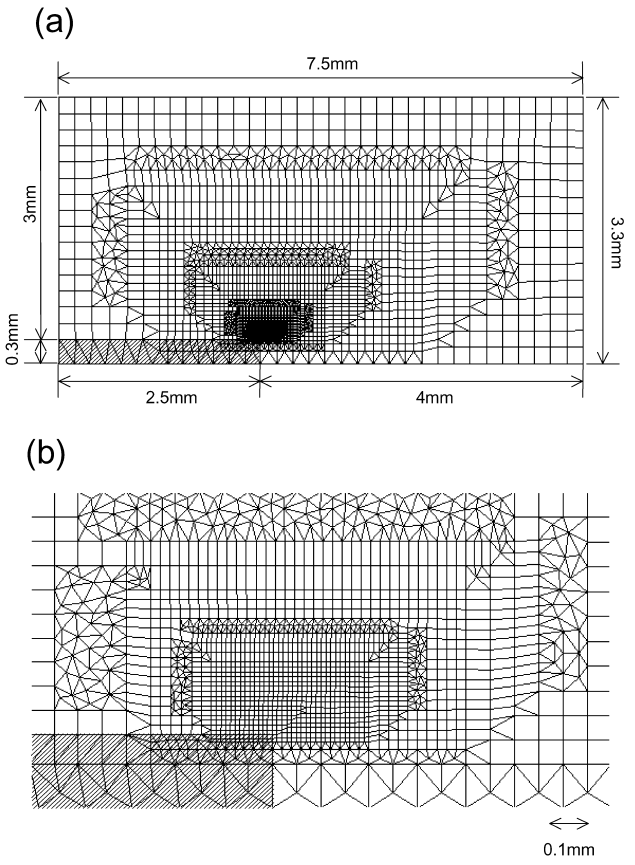

Fig. 2. Two-dimensional computational mesh used for finite element modeling. Shadowed region indicates the Si substrate: (a) Overall meshing for half of the model geometry, and (b) magnified illustration of the chip edge region.

meshes used in the calculation are shown in Fig. 2. Both quadrilateral and triangular elements were used for modeling. A larger number of elements were used at the edge of the chip as compared with the periphery of the model in order to account for possible areas with narrow stress distributions. The number of elements used for the modeling was 3754 where the largest and smallest element sizes were 200 and 7.5 μm, respectively. Material constants of each substance are listed in Table 1. Elastic Young's modulus and thermal expansion coefficients are assumed to be isotropic and constant. Numerical solutions were obtained with a commercially available finite element computer program, (SAMCEF, Samtech SA).

Table 1
Mechanical properties of the material in a model encapsulated microelectronic device (parameters were obtained by a universal testing machine and thermal mechanical analyzer; CTE stands for coefficient of thermal expansion)

Properties	Alumina/epoxy resin	Si substrate
Young's modulus (GPa)	15	188
Poisson's ratio	0.28	0.3
CTE (K^{-1})	4.3×10^{-5}	3×10^{-6}

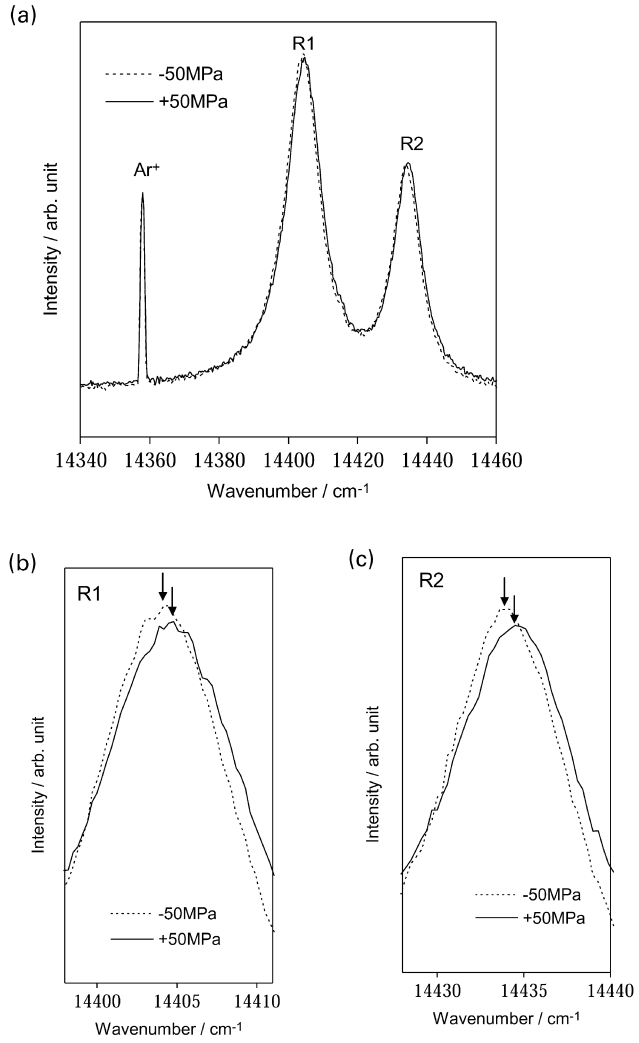

Fig. 3. (a) Fluorescence spectra of Cr^{3+} impurities in α-alumina powder compounded in epoxy resin, together with a spontaneous emission line from the Ar^{+} laser. Solid and broken lines denote the spectra under +50 MPa (tensile) and −50 MPa (compressive) uniaxial stress, respectively. (b, c) The arrows denote the peak position of each fluorescence line. Slight shifts in the position of the fluorescence R_1 and R_2 lines can be seen.

4. Results and discussion

4.1. Stress dependence of fluorescence spectra

Fig. 3 shows fluorescence spectra of the alumina filled epoxy resin under tensile and compressive stresses. Doublet fluorescence lines are observed at 14,400 cm^{-1} (R_1) and 14,430 cm^{-1} (R_2). This doublet results from a crystal field split excitation of the Cr 3d electrons when Cr atoms are substituted for Al atoms in the α-Al_2O_3. As can be seen, the fluorescence lines in compressive stress are slightly shifted to lower wavenumber as compared to that in tensile stress. The peak shift of the R_1 line between −50 and +50 MPa is about 0.4 cm^{-1}. The signs − and + indicate compressive and tensile stresses, respectively. Since the peak position of the fluorescence lines was sensitive to externally applied stress, external stresses should be transferred to the filled alumina powder through the epoxy resin matrix. This indicates the possibility of the PS technique to assess residual stresses in the polymer compound using measurements of frequency shifts of its fluorescent filler.

Fig. 4(a) shows the stress dependence of the frequency shift of the R_1 line. As seen in Fig. 4(a), the fluorescence R_1 line shifts to lower and higher wavenumber with increasing compressive and tensile stress, respectively. An

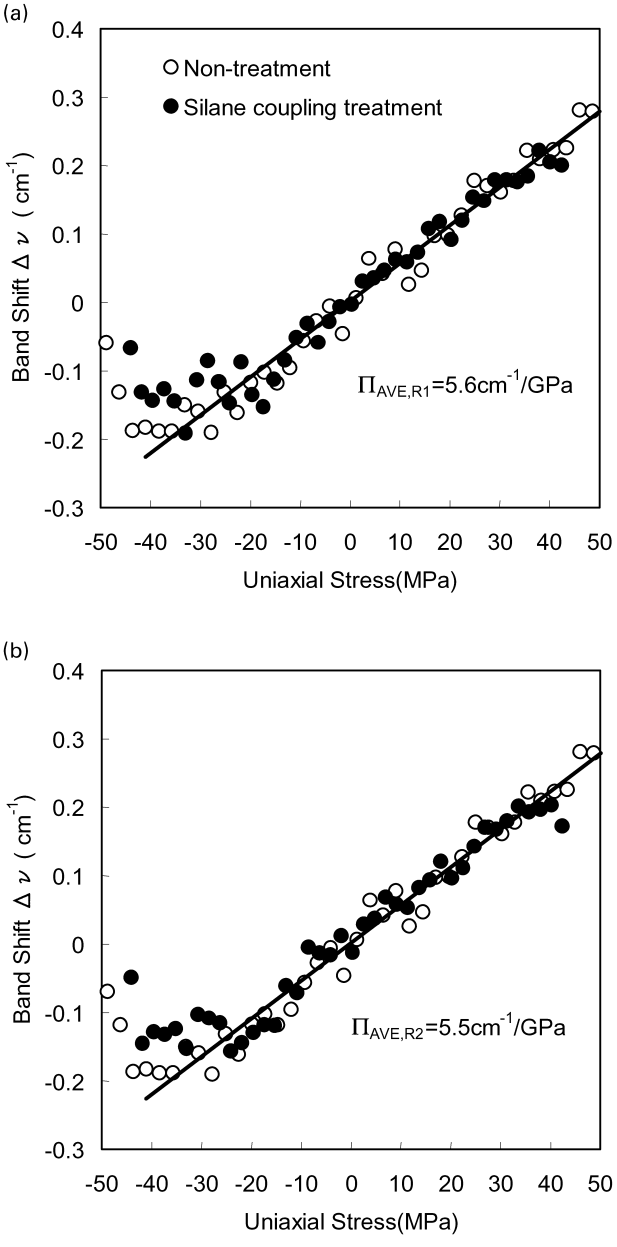

Fig. 4. Variation of the peak position of fluorescence lines with applied uniaxial stress for alumina filled epoxy resin. The PS coefficients, Π_{ave} are given by the respective average slopes of the measurement plots: (a) R_1, and (b) R_2 line.

approximately linear relationship between the shift of the R_1 line and tensile strain was obtained. The frequency shift of the non-treated sample, which contains alumina filler without silane treatment, was found to be the same as that of the sample treated with silane. This linear correlation suggests that the externally applied macroscopic tensile strain is proportional to the internal strain in the filled alumina particles. Therefore, as long as a tensile stress is considered, the shift of fluorescence lines can be directly used for stress measurement, according to a correlation coefficient. In contrast, a considerably non-linear relation between frequency shift of the R_1 line and compressive stress was found. In the compressive region, the external applied stress is no longer proportional to internal stress stored in the alumina filler. A similar behavior was also recognized in the stress dependence of peak frequency for the R_2 line (Fig. 4(b)). This non-linear phenomenon can be seen even in the small compressive stress regions, ≈ -20 Mpa. This trend was independent of whether the alumina filler was treated with silane coupling agent or not. Considering that the fluorescence lines of alumina crystal themselves are known to have a linear correlation between frequency and compressive stress to at least some hundreds of MPa [27], this non-liner phenomenon should arise from a mechanism of stress-transfer from epoxy resin to alumina particles. Because the adhesive force between surface of filler and epoxy resin should be strengthened by using the silane-coupling agent, this non-linearity does not appear due to weak adhesive strength at the interface. Though the exact cause of this non-linearity is not completely clear, we suggest here that non-linearity is related to plastic deformation occurring in the epoxy resin.

As far as tensile stresses are considered, the PS technique can be applied with high reliability to the alumina filled epoxy resin composite. The PS coefficients for this material are listed in Table 2. These values merely refer to frequency shift in the tensile stress region. Stress dependency of the R_1 and R_2 fluorescence lines for both single crystal and polycrystalline aluminum oxide has been extensively studied. The average values of PS coefficients for a single crystal are 2.53 and 2.5 $cm^{-1}\,GPa^{-1}$ for R_1 and R_2 lines, respectively [27]. The apparent PS coefficients, $\Pi_{R_1} = 5.6\ cm^{-1}\,GPa^{-1}$ and $\Pi_{R_2} = 5.5\ cm^{-1}\,GPa^{-1}$ in the present composite are almost twice as large as that for a monolithic Al_2O_3 material. This shows that the external stress concentrated in the alumina filler since the Young's modulus of the filler is much larger than the matrix resin. Stress concentration in an inclusion within a polymeric matrix has also been studied by X-ray diffraction technique [30]. It has been reported that a particle of aluminum metal in a polystyrene matrix yields almost two times the external stress in the stress direction. This factor of stress-transfer is considered to be mainly governed by the ratio of elastic moduli between filled particles and resin matrix [30].

Table 2
PS coefficients obtained for the alumina filled epoxy resin used in this study (Π_{ave} denotes the average value of the diagonal components of PS coefficients)

Sample	Π_{ave,R_1} ($cm^{-1}\,GPa^{-1}$)	Π_{ave,R_2} ($cm^{-1}\,GPa^{-1}$)
Non-treatment	5.6	5.5
Silane coupling treatment	5.6	5.5
Single crystal[a]	2.53	2.54

[a] Single crystal's values are taken from Ref. [27].

4.2. Application to a model microelectronic device

Since thermal residual stresses are expected to be concentrated at the interface between the epoxy resin and the Si substrate, the measurement has been done along a line parallel to the interface from center toward the chip edge (line A in Fig. 1). Fig. 5 shows experimental results obtained for thermal residual stresses along line A. The frequency shifts of the fluorescence line (R_1) have been divided by the PS coefficient listed in Table 1. The stress values are expected to correspond to the macroscopic average stress in the alumina/epoxy encapsulant. A stress-free spectrum has been selected at a position far away from the Si substrate. According to the thermal expansion mismatch between the Si substrate and the encapsulant resin, the resin adjacent to the Si substrate should be found to be under a tensile stress. The behavior of the tensile stress on the Si substrate is rather flat and, furthermore, a steep stress deviation has been detected at the edge of the chip. The value of the tensile stress in the vicinity of the Si substrate is around +60 MPa. According to calculations using an elastic two-layer model, Eq. (6) predicts an interfacial stress in the resin of +48 MPa, when the glass transition temperature is 125 °C. The reasonable agreement between calculated and measured values suggests the effectiveness of a simple two-layer model and its elastic assumption. The stress variation

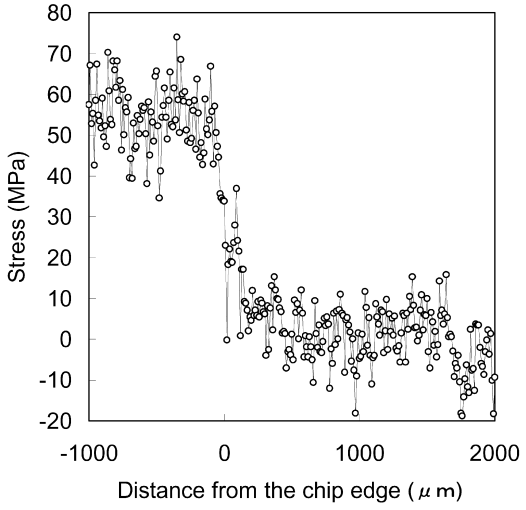

Fig. 5. Residual stress distribution obtained from α-alumina fluorescence along line A on the model microelectronic device. Measurement points from −1000 to 0 were in the vicinity of the Si substrate.

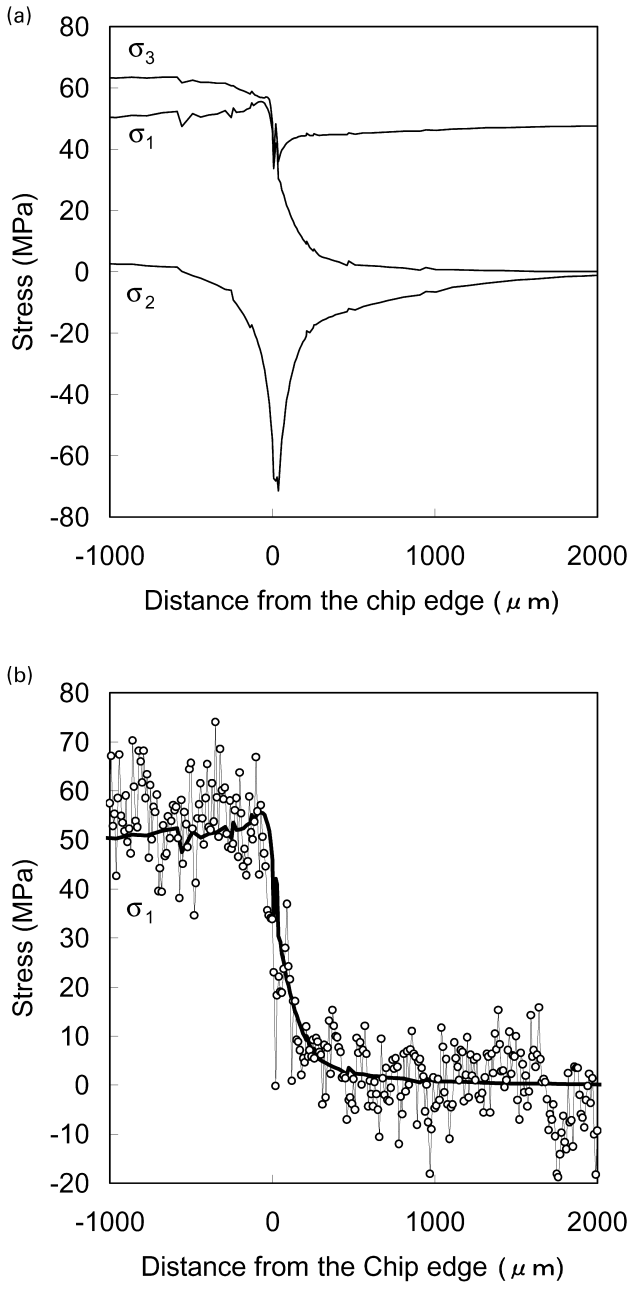

Fig. 6. (a) Stress components calculated from the FEM along line A. (b) Comparison of experimentally-determined residual stresses and the calculated in-plain tensile stress component. Solid line indicates FEM generated data.

in the matrix resin is found within 300 μm from the edge of the chip. Namely, the thermal stress induced by the existence of the Si substrate is localized at the interface. It can be seen that the measured stress values are scattered at about 10 MPa irrespective of location. Another experiment at the same line shows that the stress values are almost reproducible within a few MPa. Therefore, the deviation may be mainly caused not by a measurement error, but by the variation of concentration of alumina filler in the matrix resin and/or the inhomogeneity of the alumina filler itself.

The experimental result of the residual stress distribution along line A was compared with values calculated by FEM. Fig. 6(a) shows the three principal stress components along line A. First and second components correspond to tensile and compressive stress along the cross-section, respectively. The third component can be ignored because this component corresponds to a direction vertical to the cross-section and that might be relaxed by the cutting procedure. The directions of these three principal stress components are diagonal to each other. First and second components change these directions along line A continuously. At the center of the device, the direction of first/tensile component is parallel to the interface of Si substrate. That direction comes to be vertical to the diagonal line of Si substrate at the edge of chip. A comparison between experimental values and FEM calculations is shown in Fig. 6(b). Following expression (3), the measured stress value at the cross-section should be the average of two stress components, but the experimental result gave good agreement with only the first, namely, the tensile component, rather than with the average value of the two components. According to FEM calculation, the large compressive stress may be generated at just the edge of the chip, but the experimental results do not contain such a steep compressive stress. By assuming the frequency shift as ascribed only to tensile components, the agreement of the calculated tensile stress with data measured from PS technique is very good; both shapes of the curves and the stress magnitude are similar. This phenomenon might be related to the non-linear behavior of the frequency shift on the compressive stress side in Fig. 4. Owing to non-linearity, the frequency shift may not be sensitive to compressive stress. It is also noted that the spatial resolution of the PS technique for the alumina/epoxy encapsulant should suffice to measure the stress variation at the chip edge.

The experimental results of residual stress distribution along B and C lines are shown in Fig. 7(a) and (b), and compared to the value from the FEM calculation. Highest stresses are found in the vicinity of the Si substrate, the tensile stresses decreasing monotonically. The experimental stresses again are in a satisfactory agreement with the tensile stress component derived from FEM calculation. The agreement between experimental and calculated data may provide evidence that the frozen-in residual stresses actually originated below the glass transition temperature by thermal expansion mismatch between Si substrate and encapsulant.

Fig. 8 shows the residual stress-distribution along line A at 23 and 80 °C. The PS coefficient of the R_1 fluorescence line was the same as that at room temperature, since the PS coefficients for alumina do not depend much on temperature [27]. Tensile stresses in the vicinity of the Si substrate decrease dramatically at high temperature. This result is well explained by the reduction of the difference between the glass transition and the measurement temperatures, $T_g - T_a$ as shown in Eq. (7). The recovery of residual stresses upon cooling down to room temperature is also shown in Fig. 8. The residual stresses in the vicinity of the Si substrate

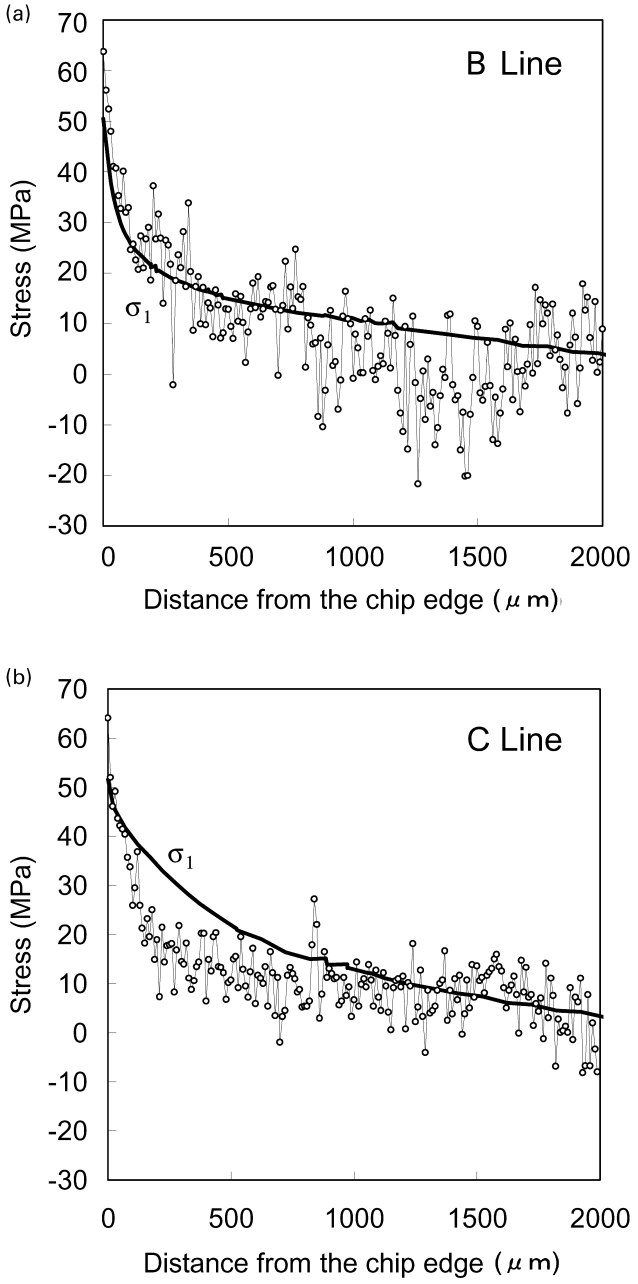

Fig. 7. Comparison of the experimental stress distribution and FEM values calculated in-plain tensile stress component: (a) along line B, and (b) line C.

recovered and slightly increased by an average of 10 MPa, as compared with experiments before heating. Increase of tensile stress may be interpreted as further hardening of the epoxy resin during re-heating which might increase the Young's modulus of the resin.

Usually a microelectronic device encapsulated with resin is thoroughly evaluated by various methods to check whether it can withstand practical and long term use. One of the methods to test reliability of plastic packages is thermal shock testing, which evaluate the durability of a package against thermal stress induced by repetitions of hot and cool cycles [9]. The sample was exposed to rapidly

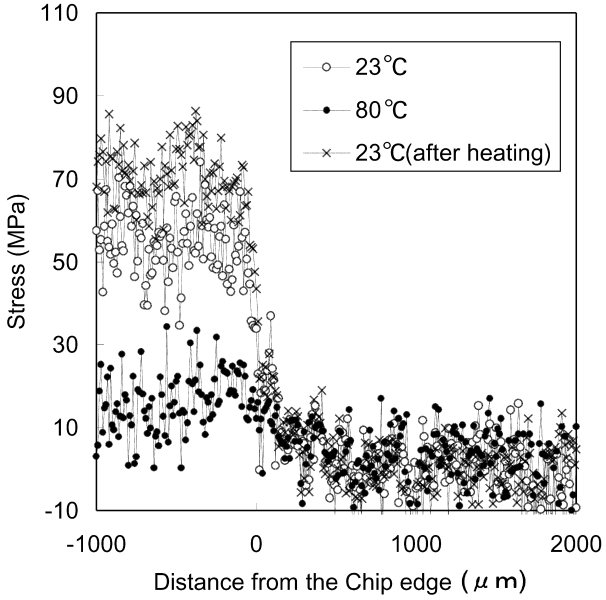

Fig. 8. Effect of a temperature change on the residual stress distribution. Measurements were performed along line A.

changing temperatures by immersing in hot (150 °C) and cold (−65 °C) silicone oil baths with a 5 min dwell time repeatedly. This is an extremely severe test for mechanical compatibility between package and encapsulant. Fig. 9 shows residual stress distributions along line A after such thermal shock testing. Residual stresses at the vicinity of the Si substrate are reduced, and the reduction of stress might be due to delamination at the interface between Si substrate and epoxy resin. Since the sample used for thermal shock testing

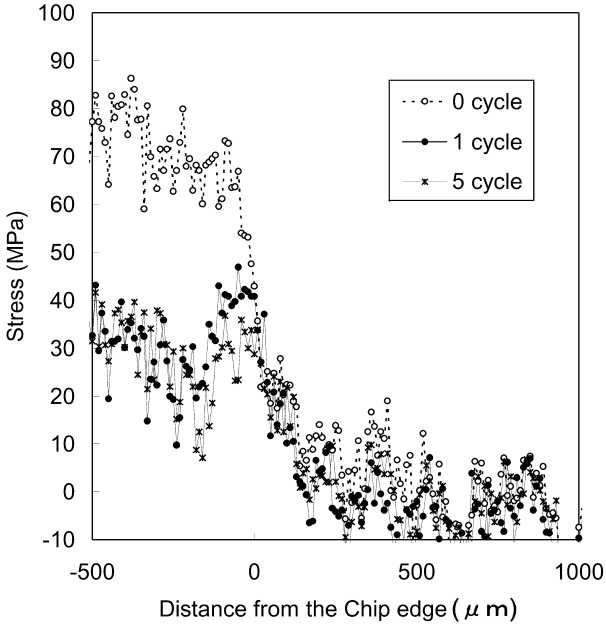

Fig. 9. Transition of the residual stress distribution during thermal shock testing along line A.

has been sectioned and the interface between epoxy resin and Si substrate is already exposed at the surface, the interface on the cross-section must be very fragile. The sudden change of interfacial stress and the weakness of the interface may cause delamination. Additionally, slightly more intense stress can be found at the neighborhood of the chip edge as compared to other interface regions. The range of the intense region is about -100 to 100 μm from the chip edge and the behavior of the stress distribution at the right side of this region does not change at all compared to that before thermal impact test. These stresses are shown to decrease and the onset of the left side of the intense region seems to be shifting during thermal cycles. The encapsulant in this region might still be in contact with the Si substrate, and gradually detaching from the substrate with repetition of heat cycles. Therefore, it is demonstrated that the adhesion of the resin to the Si substrate plays an important role in the distribution of the residual stress at the interface.

5. Conclusion

The PS method has been applied to a resin system filled with alumina particles. Stress dependence of the fluorescence line of the alumina filled epoxy resin has been studied and successfully applied quantitatively to measure the residual stress of a particle filled resin. The linear correlation between peak frequency shift and tensile stress suggest that the applied stresses definitely transfer to the alumina filler through the matrix resin. On the other hand, quite a non-linear relation between the peak frequency shift and external stresses has been found in the compressive stress region. Coefficients for peak frequency shift with regard to applied tensile stress (PS coefficients) are obtained for this alumina filled epoxy resin.

The residual stress distributions of an encapsulant around a Si substrate have been measured in a model microelectronic device and compared with values calculated by FEM. A good agreement was found between measured stress value obtained from the fluorescence technique and the tensile stress components calculated by FEM, concerning not only the shape of the stress distribution but also the stress magnitude even at the chip edge region.

As a stress measurement technique, PS is well suited to measure residual stress distributions in alumina/epoxy resin and provides very high spatial resolution when used in conjunction with an optical microscope. The technique yields detailed information for failure prediction and design improvements of polymeric products.

References

[1] Kinjo N, Ogata M, Nishi K, Kaneda A. Adv Polym Sci 1989;88:1–48.
[2] Iijima T, Horiba T, Tomoi M. Eur Polym J (a) 1991;27(9):851–8.
[3] Nakamura Y, Yamaguchi M, Okubo M, Matsumoto T. J Appl Polym Sci 1992;45:1281–9.
[4] Soane DS. Solid State Technol 1989;32(5):165–8.
[5] Suzuki H, Tabata H, Imamura N, Oizumi S. Proceedings of ASC Division of Polymeric Materials Science and Engineering, Fall Meeting, Anaheim, CA, vol. 55. 1956. p. 811–5.
[6] Okikawa S, Sizuki H. Int Symp Test Failure Anal 1984;84:180–9.
[7] Thomas RE. IEEE Trans Comp Hybrids Manuf Technol 1985;CHMT-8(4):427–34.
[8] Edwards RE, Heinen KG, Groothuis SK, Martinez JE. IEEE Trans Comp Hybrids Manuf Technol 1987;CHMT-12(4):618–27.
[9] van den Bogert WF, Molter MJ, Gee SA, Belton DJ, Akylas VR. ACS Symp Ser 1989(407):344–55.
[10] Liechti KM. Exp Mech 1985;25(3):226–31.
[11] Liechti KM, Theobald P. Proceedings of the 34th Electronic Component Conference, vol. 34. 1984. p. 203–8.
[12] Nguyen LT, Noyan IC. Polym Engng Sci 1988;28(16):1013–25.
[13] Noyan IC, Nguyen LT. Polym Engng Sci 1988;28(16):1026–33.
[14] Noyan IC, Cohen JB. Residual stress—measurement by diffraction and interpretation. New York: Springer, 1987.
[15] Yoshikawa M, Maegawa M, Katagiri G, Ishida H. J Appl Phys 1995;78(2):941–4.
[16] Wolf ID. J Raman Spectrosc 1999;30(10):877–83.
[17] Muraki N, Katagiri G, Sergo V, Pezzotti G, Nishida T. J Mater Sci 1997;32(20):5419–23.
[18] Pezzotti G. J Raman Spectrosc 1999;30(10):867–75.
[19] Wright JK, Williamson RL, Renusch D, Veal B, Grimsditch M, Hou PY, Cannon RM. Mater Sci Engng A 1999;262:246–55.
[20] Galiotis C, Paipetis A, Marston C. J Raman Spectrosc 1999;30(10):899–912.
[21] Hirai Y, Fukuda T, Kobayashi Y, Kuwahara H, Kido Y, Kubota K. Solid State Commun 1987;62(9):637–40.
[22] Wunder SL, Schoen PE. J Appl Phys 1981;52(6):3772–5.
[23] Molis SE, Clarke DR. J Am Ceram Soc 1990;73(11):3189–94.
[24] Grabner L. J Appl Phys 1978;49(2):580–3.
[25] Dauskardt RH, Ager III JW. Acta Mater 1996;44(2):625–41.
[26] Yallee RB, Young RJ. Composites A 1998;29(11):1353–62.
[27] He J, Clarke DR. J Am Ceram Soc 1995;78(5):1347–53.
[28] Och M, Tamashita K, Shimbo M. J Appl Polym Sci 1991;43:2013–9.
[29] Shimbo M, Ochi M, Arai K. J Coat Technol 1984;56(713):45–51.
[30] Hauk V. Mat-wiss u Wekstofftech 1999;30(7):377–84.